JOURNAL OF APPLIED ELECTROCHEMISTRY 21 (1991) 1063–1067

Electrodiffusional determination of momentum transfer in annular flows: axial developing and swirling decaying flows*

J. LEGRAND, P. LEGENTILHOMME, H. AOUABED

Laboratoire de Génie des Procédés, I.U.T.-BP 420, 44606 Saint-Nazaire, France

M. OULD-ROUIS, C. NOUAR, A. SALEM

Laboratoire de Mécanique des Fluides, Institut de Physique, U.S.T.H.B., Dar-El-Beida, Algeria

Received 1 February 1991; revised 28 April 1991

Two types of developing flows were studied: the axial developing flow occuring downstream of fixed beds of spheres, and the swirling decaying flow induced by a tangential inlet. In both flows, the momentum transfer was investigated for different axial distances and for a Reynolds number range of 90 to 3780 using an electrochemical method. Measurement of the wall shear stress was achieved by means of the limiting electrodiffusional current on circular microelectrodes. Comparisons of swirling flow and axial developing and developed flows are made in terms of velocity gradients and friction factors.

Notation

A	microcathode surface area
C_S	potassium ferricyanide concentration
d	microelectrode diameter
$e = R_2 - R_1$	thickness of the annular gap
F	Faraday constant
f_{ax}, f_{df}, f_e	friction factors
I_L	limiting diffusional current
k_F	local mass transfer coefficient
L_e	entrance length
R_1	external radius of the inner cylinder
R_2	internal radius of the outer cylinder
$Re = \frac{2e\,u_m}{\nu}$	Reynolds number
s_{ax}, s_{df}, s_e	velocity gradients
u_m	mean axial velocity
x	axial coordinate
ν	kinematic viscosity

1. Introduction

Entrance effects in ducts of annular geometry are of particular importance for mass and heat exchangers. Indeed, the mass or heat transfer surface often begins at the inlet of industrial devices. Firstly, we have studied the axial developing flow obtained downstream of a sphere-packed annulus with the object of investigating a uniform velocity distribution at the beginning of the transfer section. The plug flow condition is usually assumed for simultaneous development of velocity and concentration (or temperature) profiles. The differences between plug flow conditions and non-uniform velocity conditions obtained downstream of packed beds at the entrance of the annulus were previously [1] analysed by a numerical method. The second kind of developing flow was obtained by means of a tangential inlet to give a decaying swirling flow in the annulus. Swirling flow is useful in a number of engineering applications in order to improve heat exchanger or electrochemical reactor performance [2].

The hydrodynamic characteristics of these two types of developing flows were investigated by use of the electrochemical method with microelectrodes, which allowed the determination of the velocity gradient on the outer cylinder of the annulus.

2. Experimental

2.1. *Cell-electrolyte*

A schematic flow diagram is shown in [2]. The annulus test section was made of an outer tube, 600 mm long with 25.1 mm internal radius, R_2. The inner cylinder, 36 mm in diameter, consisted of five different Ni or PVC parts each 100 mm long. Two of these sections acted as cathode and anode. According to the category of developing flows studied, two different types of fluid inlet were used:

(i) *for the axial developing flow*, a second cylindrical annulus 55 mm long was placed upstream of the annular test section (Fig. 1a). The fluid entered inside the inner cylinder. Four holes allowed a uniform distribution of the flow in the annular cross-section. Then the fluid flowed through the annular packed bed of spheres of 2 mm diameter. Thus the initial velocity distribution at the entrance section corresponded to the exit of an annular porous medium [1].

* This paper was presented at the Workshop on Electrodiffusion Flow Diagnostics, CHISA, Prague, August 1990.

0021-891X/91 $03.00 + .12

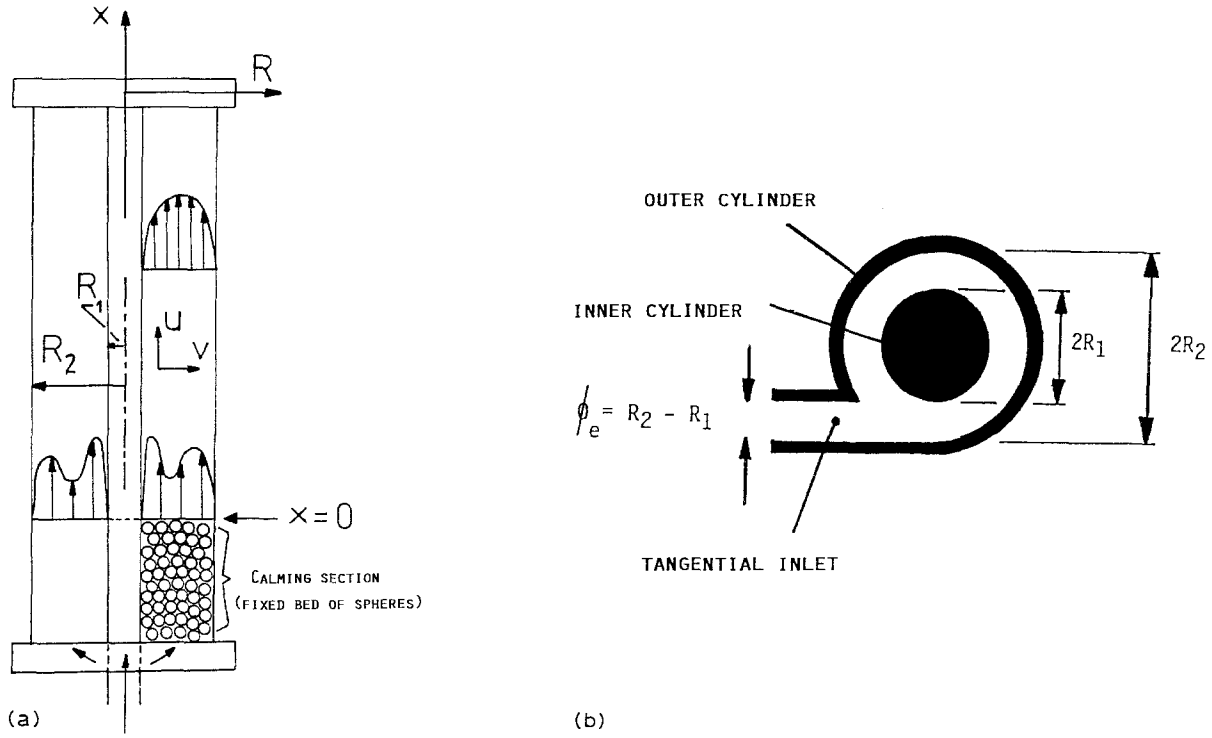

Fig. 1. Experimental arrangement: (a) for axial developing flow and (b) for swirling decaying flow.

(ii) *for the decaying swirling flow*, the initial swirl motion was induced by means of tangential inlet (Fig. 1b) equal in diameter to the thickness e ($e = R_2 - R_1 = 7.1$ mm) of the annular gap. In this configuration, the fluid movement is called pure swirl flow [3], due to the absence of a step between the inlet and the annulus.

The local electrochemical measurements were made using a polarographic method involving the reduction of ferricyanide ions at a nickel microelectrode. The electrolyte was NaOH 0.5 M supporting a mixture of 2×10^{-3} M potassium ferricyanide and 5×10^{-2} M potassium ferrocyanide. The experiments were carried out at a constant temperature of 30° C; the electrolyte density was $\rho = 1030\,\mathrm{kg\,m^{-3}}$, its viscosity $\nu = 8.73 \times 10^{-7}\,\mathrm{m^2\,s^{-1}}$ and its diffusion coefficient $D = 6.95 \times 10^{-10}\,\mathrm{m^2\,s^{-1}}$.

2.2. *Microelectrodes*

In order to obtain local information, nickel microelectrodes were placed on the outer cylinder of the annulus. 23 microelectrodes were embedded axially along the outer cylinder. Each microelectrode consisted of the cross-sectional area of a nickel wire of diameter 0.4 mm. The experimental arrangement included an electronic circuit with a multiplexer and a potentiostat, PRT 20–2. When the cylindrical surface was not electrically connected to the cathodic circuit, the mean limiting current measured at each microelectrode led to a local mass transfer coefficient, k_F. Reiss and Hanratty [4] have shown that there is a relation between k_F and the velocity gradient, s, for a circular microelectrode of diameter d:

$$k_F = \frac{I_L}{FAC_s} = 0.862\left(\frac{D^2 s}{d}\right)^{1/3} \qquad (1)$$

The calibration of the microelectrodes was made under developed annular laminar flow conditions.

3. Developing laminar axial flow

3.1. *Flow description*

When fluid enters an annular duct, a hydrodynamic boundary layer begins to develop on the walls of the annulus. As the fluid progresses downstream, the boundary layer on the inner cylinder thickens until it reaches the boundary layer from the outer cylinder. At this point, the velocity profile is quasi-established. The diffusional boundary layers on both walls develop in a similar manner up to the pure diffusion concentration profile. Generally, it is assumed in the literature that there is plug flow at the entrance to the annulus. In this paper, we have experimentally studied the simultaneous hydrodynamic and mass transfer developments by using a calming section (Fig. 1a) composed of a fixed bed of spheres. In a previous paper [1], we have shown by numerical resolution of the equations that this type of entrance condition gave different results, due to the high values of the axial velocity near the walls, in comparison with plug flow condition at the entrance.

3.2. *Experimental results*

The velocity gradients at the outer cylinder were determined in the following experimental domain: $90 < Re < 1530$ and $0.7 < x/2e < 35$. The variation of the velocity gradient, s_{df}, is given in Fig. 2a for three different values of Re. The experimental data are only correlated in the entrance region, where the decrease in the velocity gradient occurs. Downstream of the entrance region the velocity gradient is nearly constant

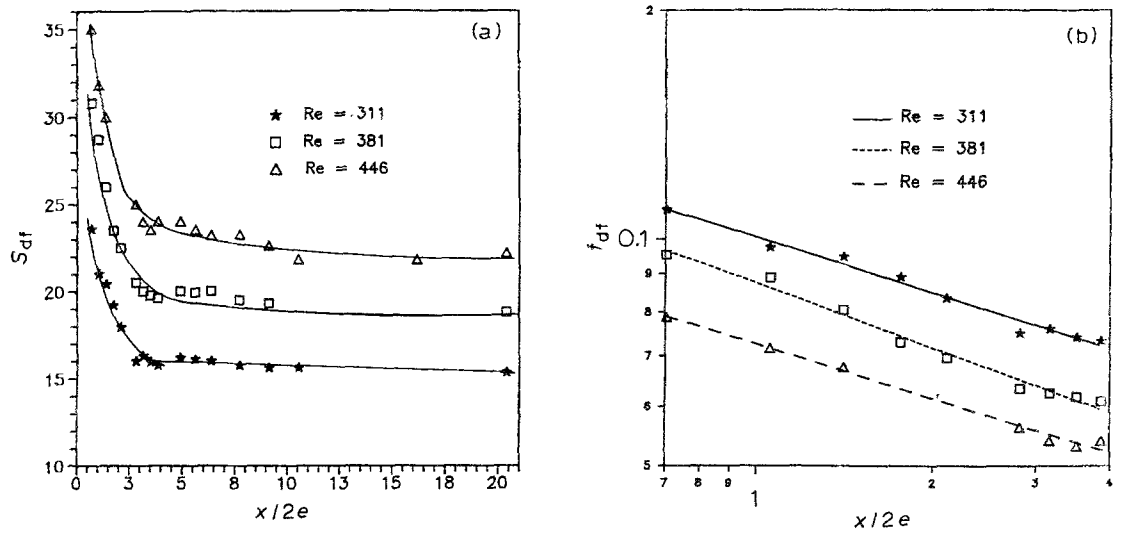

Fig. 2. Momentum transfer in axial developing flow: (a) variation of the velocity gradient with axial distance, and (b) variation of the friction factor with the dimensionless axial distance. Key for *Re*: (★) 311, (□) 381 and (△) 446 on both (a) and (b).

(Fig. 2a), and equal to the developed axial laminar velocity gradient, $s_{ax} = 0.040\,Re$ in the present experimental conditions [5]. The ratio s_{df}/s_{ax} has been correlated by a multilinear regression as a function of *Re* and $x/2e$:

$$\frac{s_{df}}{s_{ax}} = 0.39\,Re^{0.27}\left(\frac{x}{2e}\right)^{-0.32} \qquad (2)$$

The developed axial laminar flow regime is relatively quickly obtained. This result proves that fixed beds of spheres constitute an efficient calming section for obtaining developed flow. The entrance length, L_e, is determined from experimental data (Fig. 2a) by assuming that the developed axial flow is obtained when s_{df}/s_{ax} is equal to 0.99. Thus, we have obtained $L_e/2e = 0.013\,Re$. This relation is in good agreement with a previous numerical determination of L_e [1]. The momentum transfer is expressed (Fig. 2b) in terms of friction factor against the dimensionless distance $x/2e$. The data are correlated by the equation:

$$f_{df} = 7.22\,Re^{-0.73}\left[\frac{x}{2e}\right]^{-0.32} \qquad (3)$$

The decrease of f_{df} with axial distance can be represented by the parameter $(x/Re\ 2e)^{-0.32}$, which is similar to $(x/Re\ 2e)^{-0.37}$ numerically obtained by Shah and Farnia [6] for $0.003 < x/Re\ 2e < 0.02$. The latter domain corresponds approximatively to the present experimental conditions.

4. Decaying swirling flow

4.1. *Flow description*

Swirl results from the application of a tangential component to the main axisymmetric axial movement of a fluid. Such flows can be classified into two different types [7]: *continuous swirling flow* and *decaying swirling flow*. In the present work, the swirl motion is induced by a tangential inlet. The main property of this type of swirling flow is the decay of the swirl intensity along the flow path because of the decrease in tangential velocity. The swirl decay is associated with a mass transfer decrease [2, 3] with axial distance.

4.2. *Experimental results*

The velocity gradients at the outer cylinder were determined in laminar and turbulent swirling flows. The experimental domain was defined by: $90 < Re < 3780$ and $0.7 < x/2e < 35$. In Fig. 3, the experimental results are expressed in terms of s_e/s_{ax} as function of the dimensionless axial length, $x/2e$. The terms s_e and s_{ax} are the swirl and axial developed velocity gradients on the outer cylinder, respectively. For $Re < 3000$ (Fig. 3b), the axial turbulent velocity gradient, s_{ax} is obtained from [8]. In both figures, two types of velocity gradient development are seen according to the value of the dimensionless axial distance. For $x/2e < 13$, s_e/s_{ax} decreases very sharply with $x/2e$. This decrease is due to the addition of two phenomena: first, the decay of the swirl intensity and secondly, the entrance effects. The influence of the latter phenomenon is shown in Fig. 3a, giving the development of s_e/s_{df} with $x/2e$; thereby emphasizing the real swirl decay, which is also very significant in the region near the entrance ($x/2e < 13$). For $x/2e > 13$, the velocity gradient decrease is weaker and can only be related to the swirl decay. The entrance length is considerably enhanced in swirl flow as compared with axial flow. For $90 < Re < 500$ and $x/2e > 30$ (Fig. 3a), s_e is nearly equal to s_{ax}, thus the laminar axial flow regime is obtained. Otherwise, for $Re > 3000$ (Fig. 3b), the laminar regime is not established even for the farthest downstream microelectrode for which s_e/s_{ax} is greater than 2.0. The experimental data are correlated for laminar swirl by:

$$\frac{s_e}{s_{ax}} = 6.30\,Re^{0.54}\left(\frac{x}{2e}\right)^{-1.41} \qquad (4)$$

The parameters of the Equation 4 were determined by multi-linear regression, with a correlation coefficient, *r*, of 0.92. The values of the velocity gradients are sig-

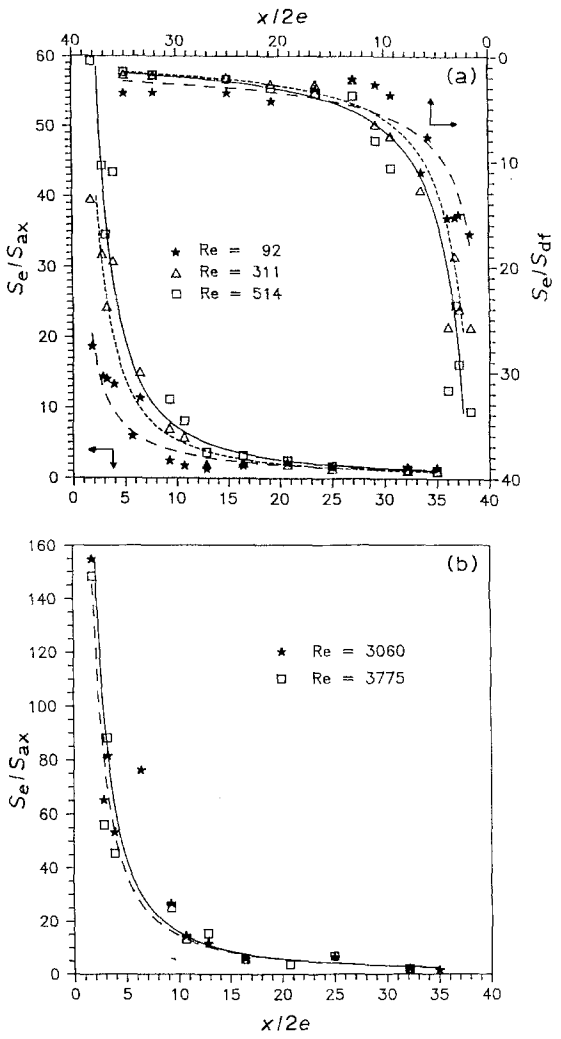

Fig. 3. Variation of velocity gradient with axial distance for swirling decaying flow (a) for $Re < 1000$: (★) 92, (△) 311 and (□) 514; (b) for $Re > 3000$: (★) 3060 and (□) 3775.

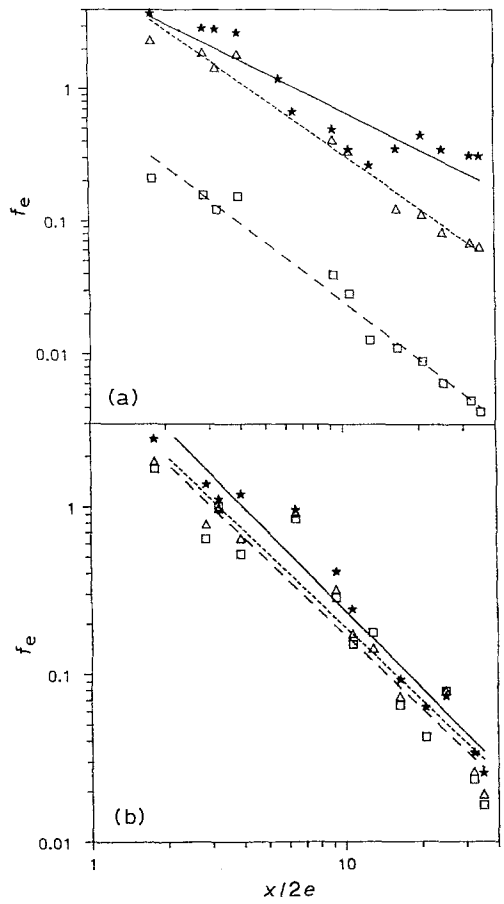

Fig. 4. Influence of axial distance on the friction factor. (a) for $Re < 1000$: (★) 92, (□) 311 and (□) 514; for $Re > 1500$: (★) 1525, (△) 3060 and (□) 3774.

nificantly higher than those obtained in axial developed flow (Fig. 3a). The real increase of the momentum transfer due to the swirl motion is obtained by taking the ratio of the swirl and the axial developing wall velocity gradients. The following equation was obtained:

$$\frac{S_e}{S_{df}} = 16.50\, Re^{0.28} \left(\frac{x}{2e}\right)^{-1.10} \qquad (5)$$

with a correlation coefficient of 0.92. Figure 4 shows the variation of f_e with $x/2e$ for laminar ($Re < 1000$, Fig. 4a) and turbulent ($Re > 1500$, Fig. 4b) flow regimes. For $Re < 1000$, the friction factor decreases with $(x/2e)^{-1.41}$ and is dependent on Reynolds number:

$$f_e = 115.7\, Re^{-0.46} \left(\frac{x}{2e}\right)^{-1.41} \qquad (6)$$

No friction factor data in laminar swirling decaying flows are available in the literature according to the present author's knowledge. It may be noted that the influence of Re is notably smaller than in laminar developed axial flow ($f_{ax} \propto Re^{-1}$) and in laminar developing axial flow ($f_{df} \propto Re^{-0.73}$, Equation 3). For $Re > 1500$, f_e is almost independent of Re (Fig. 4b), the experimental data are expressed by

$$f_e = 10.8\, Re^{-0.08} \left(\frac{x}{2e}\right)^{-1.48} \qquad (7)$$

The exponent of Re is close to that previously obtained ($f_e \propto Re^{-0.1}$) by Yukawa and Hashimoto [9] for turbulent annular swirling decaying flow induced by a rectangular tangential inlet. The decrease in the friction factor with axial distance has the same form in the laminar (Equation 6) and turbulent (Equation 7) flow regimes. This result was also obtained in mass transfer experiments [2].

5. Conclusion

The application of a tangential component to the axial movement leads to a significant increase in the entrance length: for example, for $Re = 310$, $L_e \simeq 6$ cm for axial flow and $L_e \simeq 50$ cm for swirl flow. The velocity gradient is greater when the velocity profile is not established compared with the laminar fully developed velocity distribution. Then the enhancement of the entrance length is associated with an increase in momentum transfer. The values of the friction factor are greater in swirling flow. The comparison of the friction factors obtained in axial developing flow and swirling decaying flow shows that the swirl motion leads to a decrease of the influence of the Reynolds

number, otherwise the diminution of the momentum transfer with axial distance is increased.

References

[1] M. Ould-Rouis, C. Nouar, A. Salem, J. Legrand and P. Legentilhomme, *I. Chem. Engr. Symp. Series* **12** (1989) 17.

[2] P. Legentilhomme and J. Legrand, *J. Appl. Electrochem.* **20** (1990) 216.

[3] P. Legentilhomme and J. Legrand, *Int. J. Heat Mass Transfer* **3** (1991) 1281.

[4] L. P. Reiss and T. J. Hanratty, *A.I.Ch.E. J.* **9** (1963) 154.

[5] R. P. Bird, W. E. Stewart and E. N. Lightfoot, 'Transport phenomena' John Wiley, New York (1960).

[6] V. I. Shah and K. Farnia, *Computers and Fluids* **2** (1974) 285.

[7] A. K. Gupta, D. G. Lilley and N. Syred, 'Swirl flows', Abacus Press, Tonbridge Wells, UK (1984).

[8] R. R. Rothfus, C. C. Monrad and V. E. Senecal, *Ind. Eng. Chem.* **12** (1950) 2511.

[9] H. Yukawa and M. Hashimoto, *J. Chin. Inst. Chem. Eng.* **13** (1982) 987.